

Supplemental information

Multimodal profiling of lung granulomas in macaques

reveals cellular correlates of tuberculosis control

Hannah P. Gideon, Travis K. Hughes, Constantine N. Tzouanas, Marc H. Wadsworth II, Ang Andy Tu, Todd M. Gierahn, Joshua M. Peters, Forrest F. Hopkins, Jun-Rong Wei, Conner Kummerlowe, Nicole L. Grant, Kievershen Nargan, Jia Yao Phuah, H. Jacob Borish, Pauline Maiello, Alexander G. White, Caylin G. Winchell, Sarah K. Nyquist, Sharie Keanne C. Ganchua, Amy Myers, Kush V. Patel, Cassandra L. Ameel, Catherine T. Cochran, Samira Ibrahim, Jaime A. Tomko, Lonnie James Frye, Jacob M. Rosenberg, Angela Shih, Michael Chao, Edwin Klein, Charles A. Scanga, Jose Ordovas-Montanes, Bonnie Berger, Joshua T. Mattila, Rajhmun Madansein, J. Christopher Love, Philana Ling Lin, Alasdair Leslie, Samuel M. Behar, Bryan Bryson, JoAnne L. Flynn, Sarah M. Fortune, and Alex K. Shalek

Fig S1

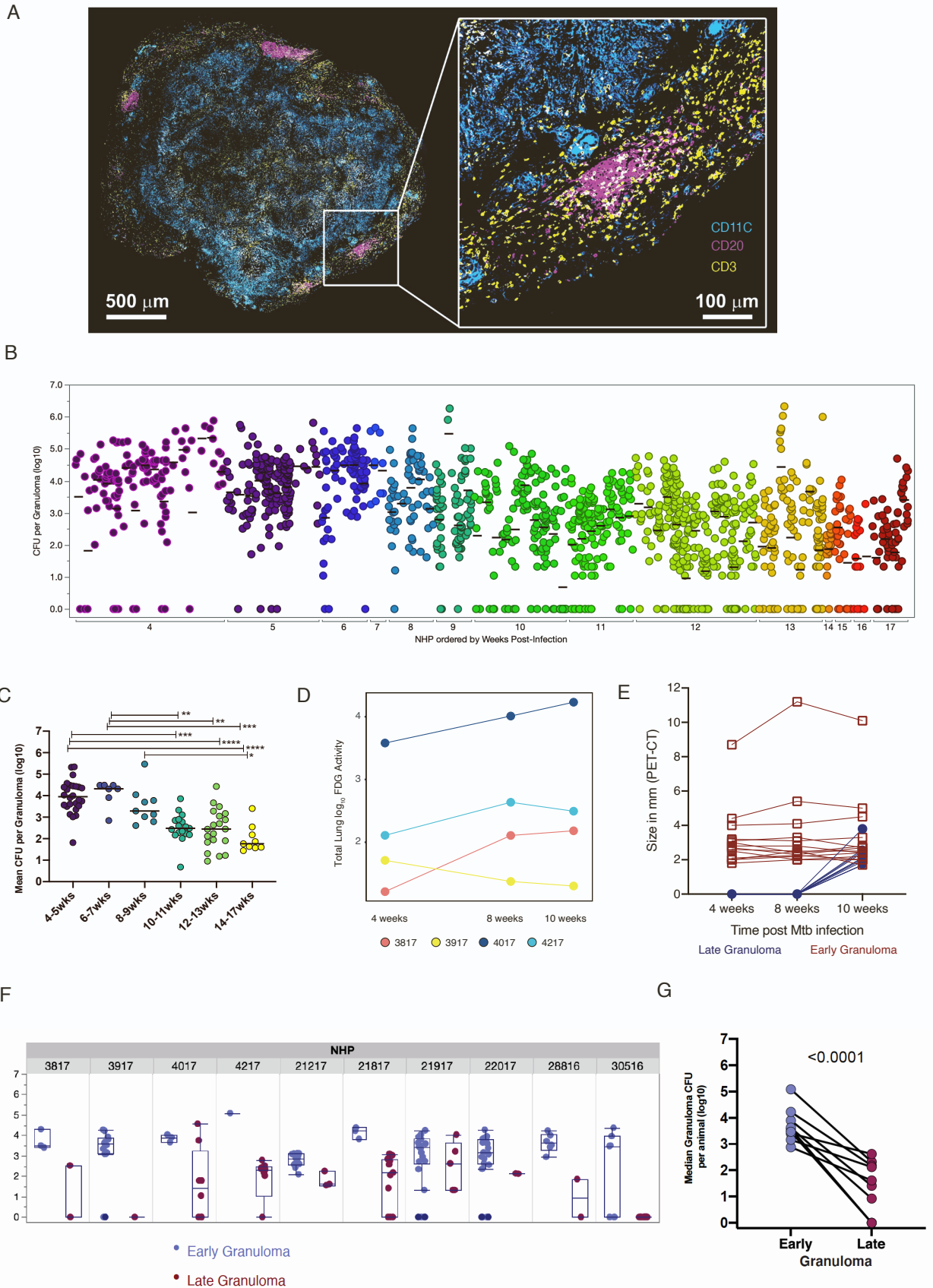


Figure S1. Characterization of granuloma architecture and bacterial burden dynamics (related to Fig 1)

(A) Architecture of macaque TB lung granuloma, where lymphocytes and macrophages are present in distinct regions. Immunohistochemistry and confocal microscopy were performed on a granuloma from an animal at 11 weeks post-Mtb infection to visualize localization of CD11c+ macrophages (cyan), CD3+ T cells (yellow), and CD20+ B cells (magenta). (B) Each column depicts the CFU for all granulomas of an individual macaque (N=88 macaques), ranging from 4 weeks to 17 weeks post-infection. Each dot represents a granuloma. Lines are at means (per animal) and different colors represent weeks post-infection. (C) CFU per granuloma decreases significantly starting at 10-11 weeks post-infection. Each dot represents the mean CFU per granuloma of an individual animal, with the x-axis indicating weeks post-infection at which necropsy was performed. Lines are at medians. Differences between time points were tested using Kruskal-Wallis test with Dunn's multiple comparison adjustment. (* $p < 0.05$, ** $p < 0.01$, *** $p < 0.001$, **** $p < 0.0001$.) (D) Total lung FDG activity (in log scale) measured by PET scans of each animal at 4, 8 and 10-weeks post-Mtb infection showing trajectories of lung inflammation. (E) Size of each granuloma measured by CT scans at 4, 8 and 10 weeks post-mtb infection. Early granulomas are those identified at 4 weeks post infection (in maroon) and late granulomas are those identified at 10 weeks post infection (in dark blue). (F) CFU per granuloma is shown for early detection (blue) and late detection (red) within each animal. Box plots lines represent the median, IQR and range Each dot represents a granuloma. (G) CFU is significantly lower in new granulomas within animals. Each dot (and line) represents the median CFU per granuloma of each animal. Statistics: paired t-test

Fig S2

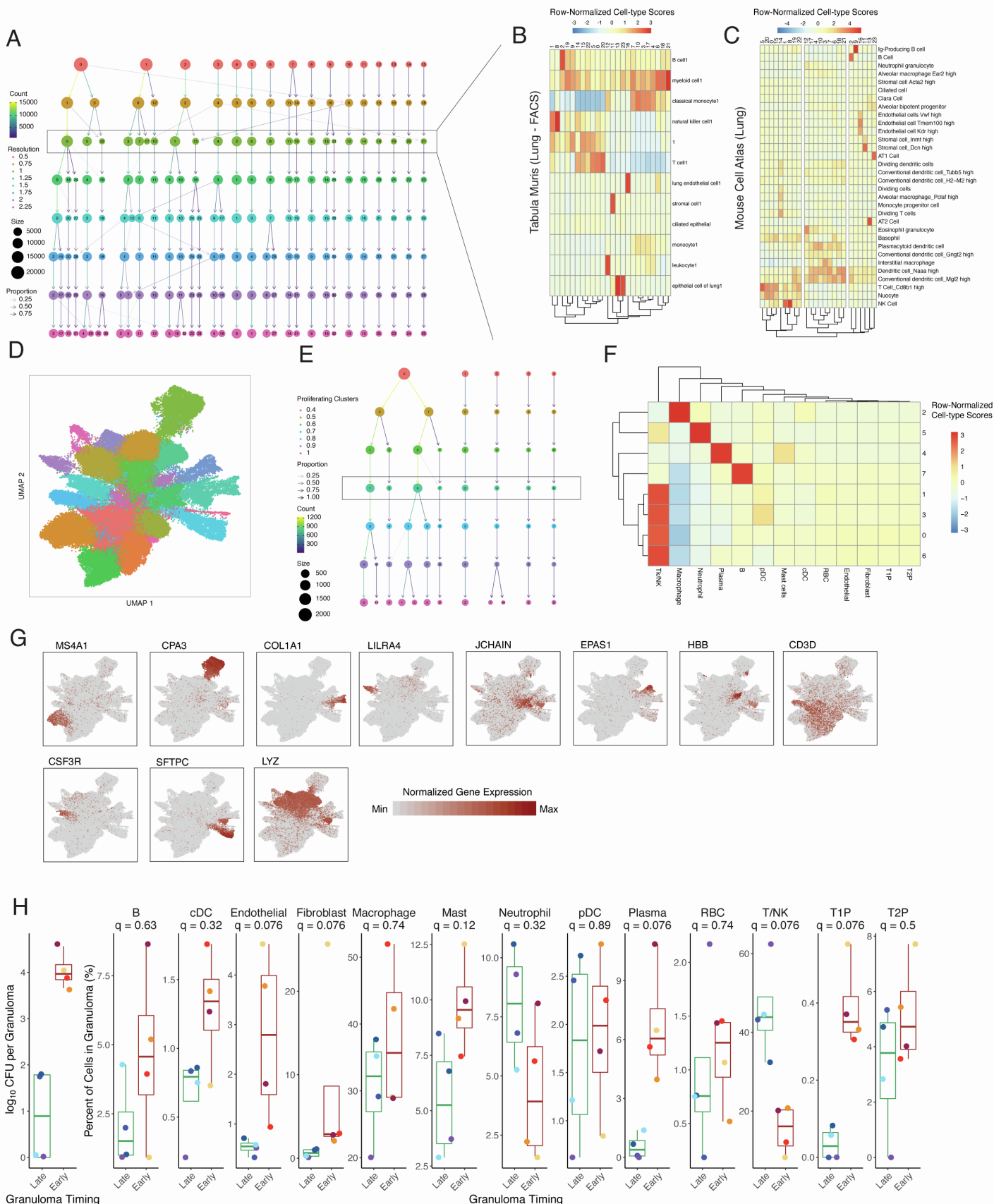


Figure S2. Identification of Canonical Cell Types (related to Fig 2)

(A) Waterfall plot showing stability of cell-type clusters at multiple clustering resolutions. Boxed row (resolution=1.00) selected for downstream analysis. **(B, C)** Distribution of lung cell-type signatures obtained from the Tabula Muris (B) and Mouse cell (C) atlas. **(D)** UMAP plot of 109,584 cells colored by Louvain clusters (resolution = 1.00). **(E)** Waterfall plot showing the stability of sub-clustering analysis of 3,123 cells with a proliferating gene signature. **(F)** Distribution of canonical cell type signatures across subclusters of proliferating cells. **(G)** Expression levels of cluster-defining genes overlaid on UMAP plot in panel 2A. **(H) Left:** CFU per granuloma based on the timing of detection by PET CT scan in one animal : 4017. **Right:** Difference in granuloma proportional composition of cell type clusters between early (maroon box plot) and late granulomas (green) within an animal (4017). Each granuloma is coloured. Statistics: Mann Whitney U test with Benjamini-Hochberg multiple testing correction. Box plot showing median, IQR and range; each dot represents a granuloma.

Fig S3

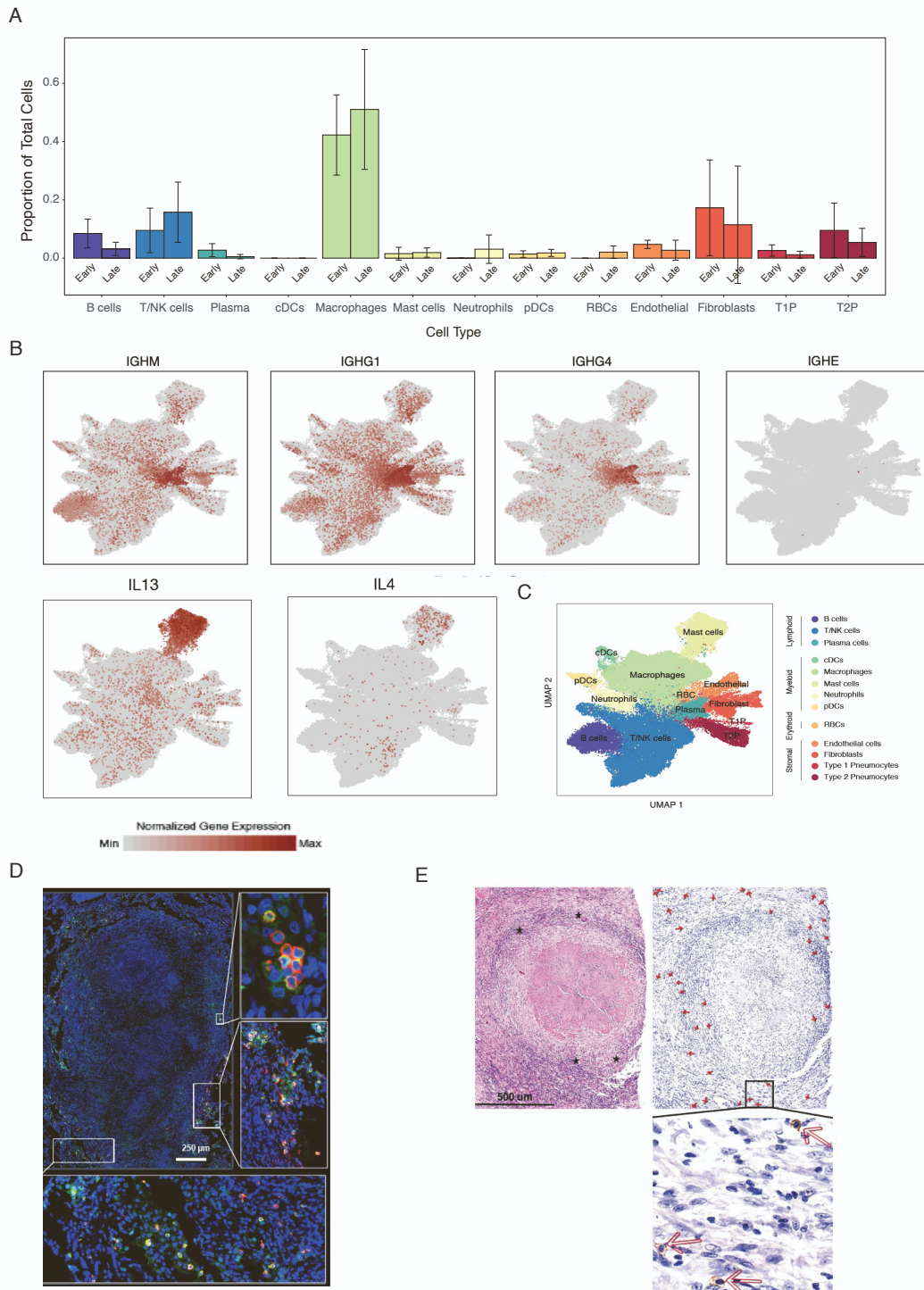


Figure S3. Cell type confirmation and Expression of selected functional transcripts (related to Fig 1-2)

(A) Proportion of cell types in granulomas from bulk sequencing of 6 early and 6 late granulomas to confirm the trend seen in scRNAseq. **(B)** UMAP plot of 109,584 cells from 26 granulomas colored by identities of 13 generic cell types. **(C)** Expression levels of select functional genes overlaid on UMAP plot of 109,584 cells. **(D)** Detection of mast cells in a 10-week NHP granuloma using immunohistochemistry, staining for tryptase (green) and c-kit (CD117)(red). **(E)** Detection of mast cells in a human lung granuloma. Hematoxylin and eosin stain and immunohistochemistry with multinucleated giant cells (stars, (top left) and c-kit (CD117) staining (indicated by arrows, top and bottom right).

Figure S4. Sub-clustering and phenotypic identification of T/NK cell populations (related to Fig 3-4)

(A) UMAP plot of 44,766 T/NK cells with a sub-cluster of 3,544 T/NK cells defined by residual contamination highlighted (blue). **(B)** Waterfall plot showing the stability of T/NK cell sub-clustering following removal of contaminated T cell sub-cluster. Boxed row (resolution=0.75) selected for downstream analysis. **(C)** T/NK subclustering UMAP overlaid with normalized gene expression for CD4, CD8A, and CD8B (top). Expression of these genes across 13 sub-clusters (bottom) where color intensity corresponds to level of gene expression and size of dots represents the percent of cells with non-zero expression in each cluster. **(D)** Frequency of expression of *CD4* (blue), *CD8A* and/ *CD8B* (green), *CD4* and *CD8A/B* (orange) or no expression of *CD4/CD8A/B* (yellow) across 13 T/NK cell subclusters. **(E)** UMAP plots overlaid with normalized expression levels for selected T/NK cell subcluster-defining genes. **(F)** Expression of key T cell markers on subclustered stem-like T cell population. **(G)** Gating Tree showing identification CD8ab T cells in lung granuloma samples and population of Granzyme A, Granzyme B and Granzyme K + CD8abT cells. **(H)** Frequency of CD8ab T cells in lung granulomas making one or more (two , three) types of Granzymes (A, B or K). Each symbol is a granuloma and each colour identifies an animal. This data supports different types of granzyme producing cytotoxic cells identified in scRNAseq.

Fig S6

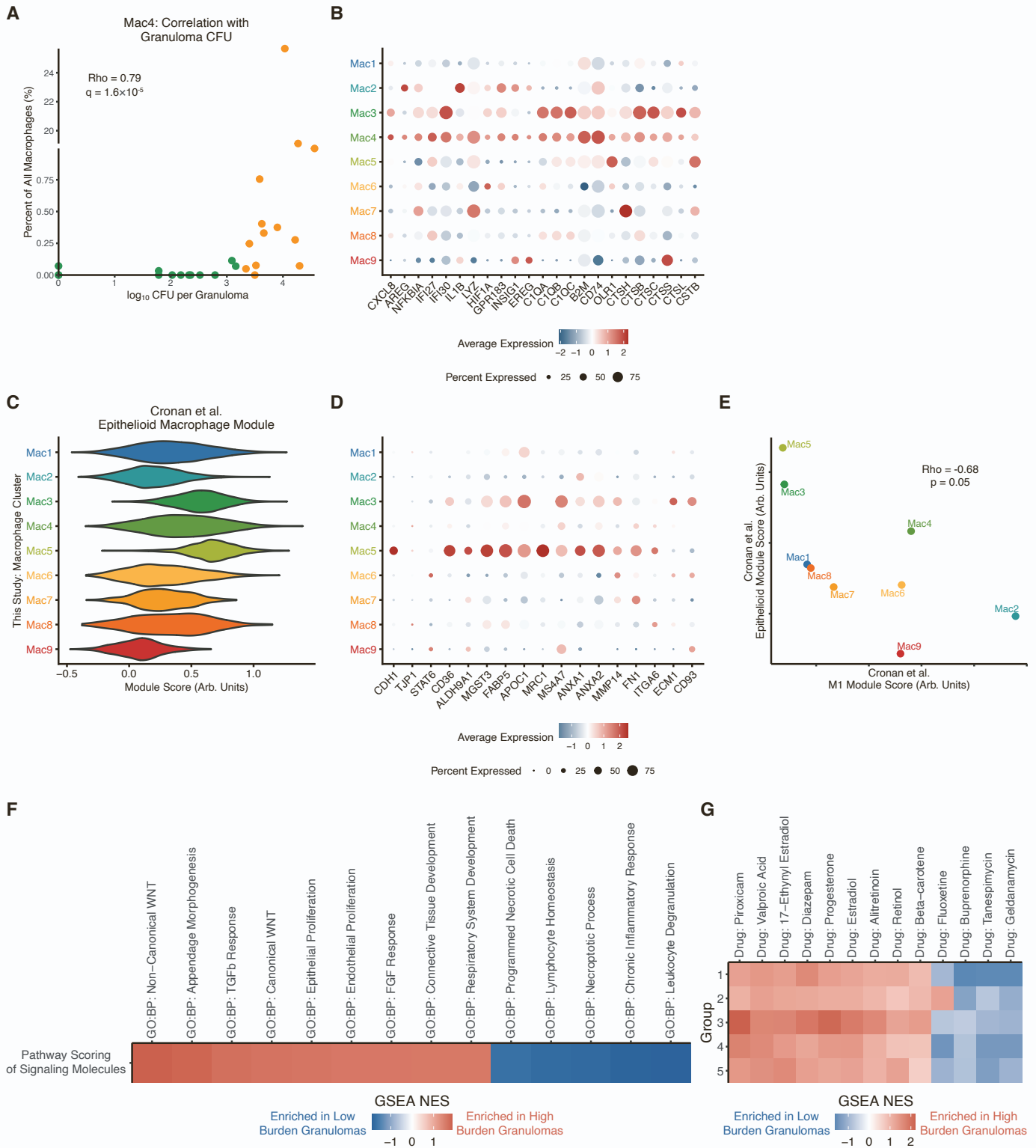


Figure S6. Connecting cell states and interactions to prior knowledge (related to Fig 2, 6)

(A) Correlation between Mac4 compositional abundance and granuloma burden, using Spearman's rho correlation test with Benjamini-Hochberg correction for multiple hypothesis testing. **(B)** Expression levels marker genes that align the Mac4 subcluster with pro-inflammatory, interferon-responsive macrophages, as in Esaulova et al. Color intensity corresponds to level of gene expression, and size of dots represents the proportion of cells with non-zero expression in each cluster. **(C)** Module scoring of macrophage clusters from this study against markers associated with Cronan et al.'s epithelioid macrophage populations. **(D)** Expression levels marker genes that align the Mac3 and Mac5 subclusters with epithelioid, pro-remodeling macrophage phenotypes, as in Cronan et al. Color intensity corresponds to level of gene expression, and size of dots represents the proportion of cells with non-zero expression in each cluster. **(E)** Module scoring of macrophage clusters from this study against M1 and epithelioid gene modules from Cronan et al; Spearman's rho correlation test. **(F)** Pathways enriched in signaling molecules associated with high vs. low granuloma burden. Signaling molecules were ranked according to their log(fold-change in high vs. low burden granulomas) as input to GSEA. **(G)** Drugs with targets enriched in signaling molecules associated with each cell type group.